the general science journal

Doppler factoring of Gaussian gravitational flux

J.C. Sands – sandsjc@shaw.ca

Abstract

The relativistic Doppler effects are merged with Gauss's gravitational flux theorem in order to model the gravitational flux distribution of moving masses. The relativistic Doppler equations accommodate the encoding of directional information and together with Gauss's flux equation for gravitation are able to directionally re-distribute gravitational intensity beyond its Gaussian surface.

Similar to synchrotron radiation, which sheds electromagnetic energy in a concentrated beam, it seems inconceivable that there is not a corresponding accompaniment of gravitational energy shed at the same time and in the same manner.

This concept, applied to rotating masses reveals a Lorentz-like effect and an asymmetric distribution of gravitational intensity; more intense on the equatorial plane and diminishing at the poles. Gravitational intensification from linear motion is found to be in the direction of motion.

Likewise for a massive concentration of orbiting objects within a galaxy, the increase of gravitational intensity outside and forward of each orbiting mass element would result in a spatially well distributed outwardly increasing gravitational gradient as distance from the galactic center increases.

A visualization of relativistic Doppler precession on rotating rings due to the Doppler displacement of the center of gravity is presented as it mimics certain orbital tendencies.

Keywords: gravitation, Doppler effect, Lorentz force, galaxy rotation, gravity assist.

1. Introduction

The concept of velocity dependent gravitation is not new. Heaviside in 1893 provided a conceptual treatment of a case in which the sun has a velocity in respect to the earth [1].

The theory of matter waves initiated in 1924 by de Broglie [2], brought insight into the wave nature of matter and how its motion exhibits wave characteristics. As well, the transformation of electron mass to electromagnetic wave energy and vice versa, points to an alternate conception of the nature of matter. Re-characterizing the macroscopic understanding of mass to a microscopic oscillatory electromagnetic substance within a transmissible medium provides the rationale to investigate and extend other wave behavior to matter, momentum and gravitation.

Einstein in his 1905 paper [3], modified the behavior of the Doppler phenomena [4] and aberration to incorporate the effects of special relativity. The paper revealed that both the frequency and amplitude of electromagnetic waves are dependent on velocity and direction and required relativistic correction. Incorporating the relativistic Doppler corrections into Gaussian gravitational formalism enables tracking of the vectored gravitational energy flux.

The notion of motion dependent gravitation can be argued starting with an interpretation of the energy momentum equation, as all energy and momentum, linear, rotational, vibratory, bound or otherwise, is contributory to the gravitational and inertial response. In 1906, Planck [5] amongst others extracted the following energy-momentum-mass relation from the principals of special relativity.

$$E^2 = p^2c^2 + m^2c^4 \qquad (1)$$

Gravitational flux with all energy as its source, E^2, includes a vectorial momentum contribution that would elicit directional gravitational flux and intensity variations in Φ_g & I_g when Doppler behaviour is considered.

Total energy versus vectored momentum; approaching and receding;

An approaching mass; $E^2{}_{(\,approaching\,)} = m^2c^4 + p^2c^2{}_{(\,approaching\,)}$ *(2)*

A receding mass; $E^2{}_{(\,receding\,)} = m^2c^4 - p^2c^2{}_{(\,receding\,)}$ *(3)*

For a receding mass; if $p^2c^2 = m^2c^4$ then $E^2 = 0$ *(4)*
as momentum energy cancels completely the rest mass energy.

The consequence of directional broadcasting of energy flux is that the faster a mass recedes from a test mass, the greater is the reduction of rearward gravitational energy as Eq. 3 would suggest. At the speed of light there will be no rearward evolution of gravitational energy.

2. Anisotropic kinematics of gravitation due to Doppler and beaming effects

Consideration is now given to the entire range of relativistic Doppler and beaming effects on linear and rotational motion. Doppler factoring is central in the study of astrophysical objects, AGNs, quasars and blazar jets but seldom to gravitation.

Following Johnson & Teller's and Einstein's similar factoring for Doppler frequency and amplitude [6][3], a factor of Γ^1 for frequency and Γ^2 for amplitude is applied for a combined Doppler factor of Γ^3. The equation below for Gauss's gravitational flux is for a uniform distribution of mass flux [7].

2.1 Gauss's law for gravity;

$$\Phi_g = \oiint_{\partial v} g.dA = -4\pi GM \qquad (5)$$

Φ_g, is the mass-energy flux enclosed by a Gaussian surface. The dA is the area factor of the infinitesimal surface elements. Little g is the gravitational intensity, I_g , passing through the Gaussian surface; assumed to be a uniform distribution out of and perpendicular to a spherical surface, however other Gaussian surface geometries and distributions are permissible, a Bouguer plate for example.

2.2 Re-arranging for I_g;

$$I_g = -\frac{\Phi_g}{A} = \frac{-4\pi GM}{4\pi r^2} = -\frac{GM}{r^2} \qquad (6)$$

The formula is now arranged to incorporate the effects of both the relativistic Doppler and relativistic Doppler beaming effects which modify the direction and intensity of I_g; for the motion generated gravitational flux.

3. Basic relativistic Doppler factor

The relativistic Doppler factor, Γ^1, in general form for every alignment is;

$$\Gamma^1 = \gamma^{-1}\left(1 - cos\,\theta_r \frac{v}{c}\right)^{-1} \qquad (7)$$

The convention adopted here is that θ is zero when the masses are moving towards each other.

The development of matter wave theory supports the application of Doppler theory. The de Broglie matter waves approaching from a moving mass would be received at a higher frequency, and higher energy content according to the basic relativistic Doppler effect. The relativistic Doppler factor, Γ^1 alters frequencies and energy, and in such, also gravitational flux.

The received frequency of an approaching mass is then $f_r = f_s\,\gamma^{-1}\left(1-\cos\theta_r\frac{v}{c}\right)^{-1}$ and the effective received wave frequency energy is $hf_r = hf_s\,\gamma^{-1}\left(1-\cos\theta_r\frac{v}{c}\right)^{-1}$ whose energy affects gravitational intensity – *in that particular direction*.

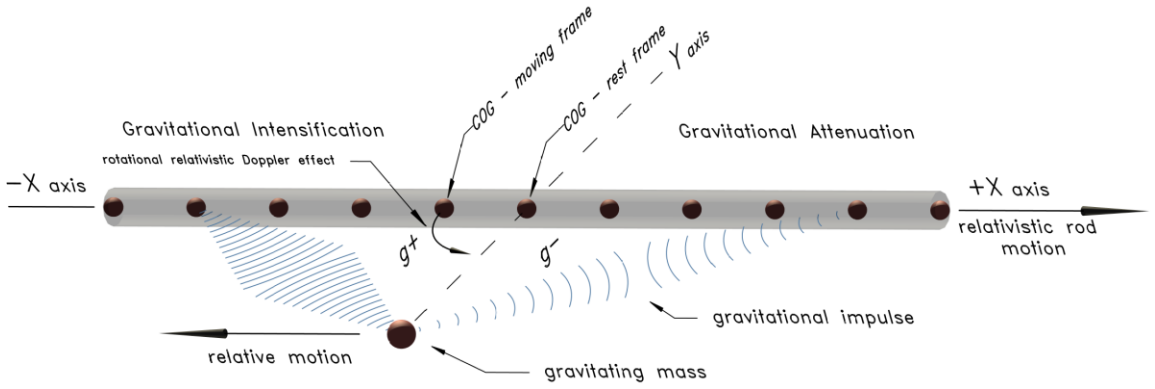

Figure 1*: Illustrates the single Γ^1 Doppler factor, $\Gamma^1 = \gamma^{-1}\left(1-\cos\theta_r\frac{v}{c}\right)^{-1}$, which increases frequency of the received gravitational impulse, producing compressed gravitational flux towards the -X axis and decompressed flux on the receding +X axis.*

The Doppler frequency modification above does not yet consider the amplitude component of the relativistic Doppler effect as described by Einstein and Johnson & Teller [3][6].

4. Relativistic beaming factor

The Doppler beaming factor, Γ^2, relating to wave amplitude in the direction of motion functions to concentrate the entire gravitational flux into smaller solid angles in the direction of motion.

In wave theory, *intensity* is proportional to the *square of the amplitude.* The increase of wave energy amplitude in relativistic Doppler factored equations ideally represents the increase of forward directed energy due to motion. Johnson & Teller [6] applied a squared Doppler factor, Γ^2, to the solid angle for beaming, $d\Omega = \mathrm{d}\Omega'/\,\Gamma^2$, as the governing angles, θ & φ, attenuate with velocity. Analogously, it must be applied to the gravitational flux of a moving mass as it concentrates amplitude energy into an ever-decreasing solid angle towards the direction of motion. If A^2 is the rest amplitude energy of a gravitating object, then the moving vectored amplitude energy is:

$$A'^2 = A^2.\Gamma^2 = A^2\,.\gamma^{-2}\left(1-\cos\theta_r\frac{v}{c}\right)^{-2} \qquad (8)$$

This is comparable to the focusing of Luminous Flux, Lumens, (lm), into fewer steradians, increasing the Luminous Intensity, Candelas, (lm/sr), in a subsequently reduced solid angle.

As Einstein [3] noted for light complexes, when v = c, *"no energy passes through the surface elements of a spherical surface moving with the velocity of light", "this surface permanently encloses the same light complex"*. Equivalently, no gravitational flux energy would be able to extend beyond a gravitational Gaussian surface element at c.

If a test mass and observer are within a focused solid angle of gravitational flux, they will perceive an amplified gravitational response. Conversely, an observer peripheral to the focused flux will barely detect a relativistic object pass when the velocity of the source approaches c.

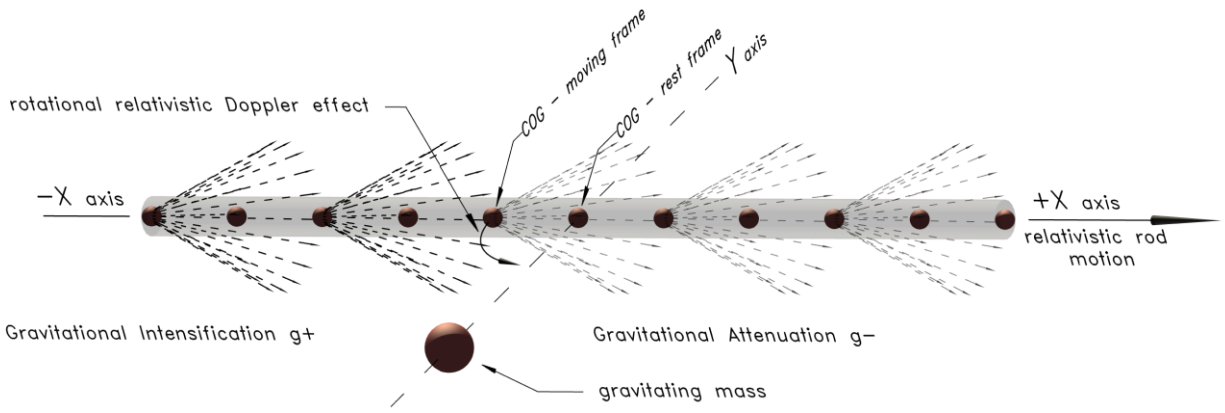

***Figure 2**: Illustrating the Γ^2 Doppler factor, $\Gamma^2 = \gamma^{-2}\left(1 - cos\,\theta_r \frac{v}{c}\right)^{-2}$, which appears to concentrate the amplitude of the gravitational flux into an increasingly focused forward solid angle as seen by the gravitating mass.*

5. Combined relativistic Doppler factor – part 1

The combined relativistic Doppler effects on longitudinal wave compression and amplitude are compounded within the reduced solid angle in the forward direction as observed by the gravitating mass; characterized as "beaming". The combined Γ^3 factor regulates the magnitude and directional distribution of the entire gravitational energy flux of the moving mass.

5.1 The Combined Doppler Factor, Γ3

$$\Gamma^3 = \gamma^{-3}\left(1 - \cos\theta_r \frac{v}{c}\right)^{-3} \tag{9}$$

Then;
$$\boldsymbol{I_{gd} = -\frac{\Phi_g}{A}.\Gamma^3} \tag{10}$$

Expanded; $$I_{gd} = -\frac{\Phi_g}{A}.\Gamma^3 = -\frac{GM}{r^2}.\gamma^{-3}\left(1 - \cos\theta_r \frac{v}{c}\right)^{-3} = -\frac{GM}{r^2}\frac{\left(1-\frac{v^2}{c^2}\right)^{3/2}}{\left(1-cos\,\theta_r\frac{v}{c}\right)^3} \tag{11}$$

6. Combined relativistic Doppler factor – part 2

The Γ^3 factor so far only accounts for the increase or decrease in directional gravitational intensity. Consideration is now given for aberration, emission location and vacuum permittivity.

The angle of incidence requires factoring for aberration [6] when the angle of incidence is not zero or 180 degrees.

6.1 Aberration factors where required

$$cos\,\theta_r = \frac{cos\,\theta_s + \frac{v}{c}}{1 + cos\,\theta_s\frac{v}{c}} \tag{12}$$

Eq. 12 will be used in Section 8 to establish the aberration experienced by the moving rod with angular inputs from the gravitating source mass, θ_s.

6.2 Gravitational intensity adjusted for emission location

The local gravitational intensity within a region is made up of impulse from a position where the source mass *was*, (r'), not where it *is*, (r), in the present. An adjustment for emission location is required to quantify the gravitational intensity and direction of action in a region of consideration.

The distance from the location of the point of emission versus its present position *for a linearly moving object* is:

$$r' = r + v\,\Delta t \;\; and \;\; \Delta t = \frac{r}{c}$$

The past divergent area factor is represented by $r'^2 \;\; where \;\; r' = r\left(1 + cos(\theta_r)\frac{v}{c}\right)$

$$\boldsymbol{I_{gd}} = -\frac{\boldsymbol{\Phi_g}}{\boldsymbol{r'^2}}\boldsymbol{\Gamma^3} \qquad (13)$$

The stationary receiver uses the θ_r angle and r'^2 factors to identify the local intensity in its stationary frame due to the moving source; above.

$$\boldsymbol{I_{gd}} = -\frac{\boldsymbol{\Phi_g}}{\boldsymbol{r^2}}\boldsymbol{\Gamma^3} \qquad (14)$$

The moving receiver uses the θ_r angle and r^2 factors to identify the sensed intensity in its moving frame due to the stationary mass; as the stationary mass has pre-established its gravitational field through which the moving mass is traversing.

As can be seen with Eq. 13, the beaming component Γ^2 may compensate for the effect of the divergent area factor r'^2.

For an optical analogy; as commented by Johnson & Teller [6], "*It is a common occurrence in optics that the diminishing intensity of a light source with increasing distance may be compensated by an increase in directionality*".

6.3 Consideration for permittivity of the vacuum

By axiom, as the gravitational impulse propagates through free space at the same velocity of electromagnetic waves; transmissibility should be considered also for gravitation. The maximum velocity of energy transmission is the speed of light, c, in a vacuum, $c = \frac{1}{(\mu_0\varepsilon_0)^{1/2}}$. Should variance in the permittivity of the vacuum be in play, ε_0 should be factored by the relative permittivity, ε_r, to determine the group wave speed of the disturbances moving through it, c_r.

$$c_r = \frac{1}{(\mu_0\,\varepsilon_r\varepsilon_0\,)^{1/2}} \qquad (15)$$

The permittivity adjusted speed of energy flux transmission, c_r, would then be used in Eq. 12-14 wherever c appears, *if warranted*. The velocity for the transmission of wave energy then becomes c_r.

With a higher ambient permittivity, (slower c), with the gravitational source continuing to produce flux at the same rate, the evolving gravitational flux depositing per unit volume is seen to increase. The wave's group velocity now being slower is offset by an increase in the wave number within the volume. A stationary observer will still sense the same number of group wave impulses pass per unit time.

The Γ^3 factor does not produce a higher gravitational intensity for the non-moving receiving mass within the higher permittivity when $\frac{v}{c_r} = 0$. The additional intensity comes into play when a mass moves through the region containing a higher wave number.

By including Doppler and aberration effects, the Gaussian approximation of gravitational intensity in a particular region can now be modeled more accurately.

Where might such directional gravitational anisotropy be evident? a) during gravity assist and flyby maneuvers, b) in increased gravitational gradients evident in anomalous galaxy rotation, c) in anomalous blazar jet deceleration and collimation due to the cumulative Doppler intensification of directional gravitational flux within the beaming jet cone, d) precession in general and orbits in specific.

6.4 Flyby and gravity assist optimization

Considering that the gravitational flux and intensity is most pronounced in front of and surrounding the equatorial plane of a rotating sphere and most diminished on the polar axis, specific approach and departure trajectories may become preferred; *as concluded in Section 11*. An approach close to the equatorial plane will enhance acceleration while egressing more towards a polar azimuth will retain more of the gains. Approach and departure trajectories on similar latitudes will be less affected.

After the gravity assist maneuver of Pioneer 10, the satellite, for a time, continues through a region where the flux augmentation, gravitational shockwave, from Jupiter was most significant; just outside and forward of its orbit trajectory. Dopplers original drawing, Fig. 7, in Appendix 1 highlights this concept visually.

A crude estimate at two hundred million kms past the Jovian intersect gave a temporal sun oriented "pull-back" in the low 10^{-10} m/s^2 over Newtonian gravity. Although not the entire amount of the anomaly looked for, but within the same magnitude; (10^{-10}).

6.5 Galactic rotational anomaly

Applying the Doppler Gravitational effect which intensifies the gravitational response outside and forward of a single orbiting object, like Jupiter, to a massive concentration of orbiting objects of a galactic plane, would result in a spatially well distributed incremental gravitational gradient increase, as distance from the galactic center increases. At 250 km/s rotational velocities, there would be noticeable changes to the inward gravitational intensity, "pull-back", which would support higher than expected rotational velocities.

7. Doppler factor, Γ^3, vs velocity

The graph below of the combined Doppler factor, Γ^3, vs velocity of selected angles of incidence reveals how the phenomena of Doppler frequency and Doppler Beaming compete at various velocities.

It is seen that the Γ^3 factors rise to a finite value of $1/(1-cos^2\,\theta)^{\frac{3}{2}}$ $at\ c.cos\,\theta$ and then decay towards zero. Even for small deviations from a directly aligned approach, the Γ^3 factor will fall towards zero when velocities approach c. When v = c, both the nominator and denominator of the Γ^3 factor reach zero simultaneously, thus avoiding an objectionable infinity and impossible physical outcome. The Doppler factors must return to zero as per Einstein's deduction stated in Section 4.

Should the relativistic Doppler effect of Eq. 7 be representative and analyzed for $\cos(\pi/2)_r$ at any tangential instantaneous velocity of the emitter, the receiver will calculate a redshift; which has the potential to be confused with redshift from a receding motion.

From the graph, it is seen that the Γ^3 Doppler factor returns to "*apparent*" redshift territory for the plotted angles at higher positive velocities even when an emitter is approaching. This happens when $\Gamma^3 < 1$

As Γ^3 is the entire relativistic Doppler energy factor made up of frequency and amplitude, what occurs is that the denominator, Γ^3, which is to the third power, at some point dominates to reduce overall directional energy transmission for the angle of incidence being evaluated. A blue shifted frequency may still be noted; however, the total directional energy attenuates faster after $c.cos\,\theta$.

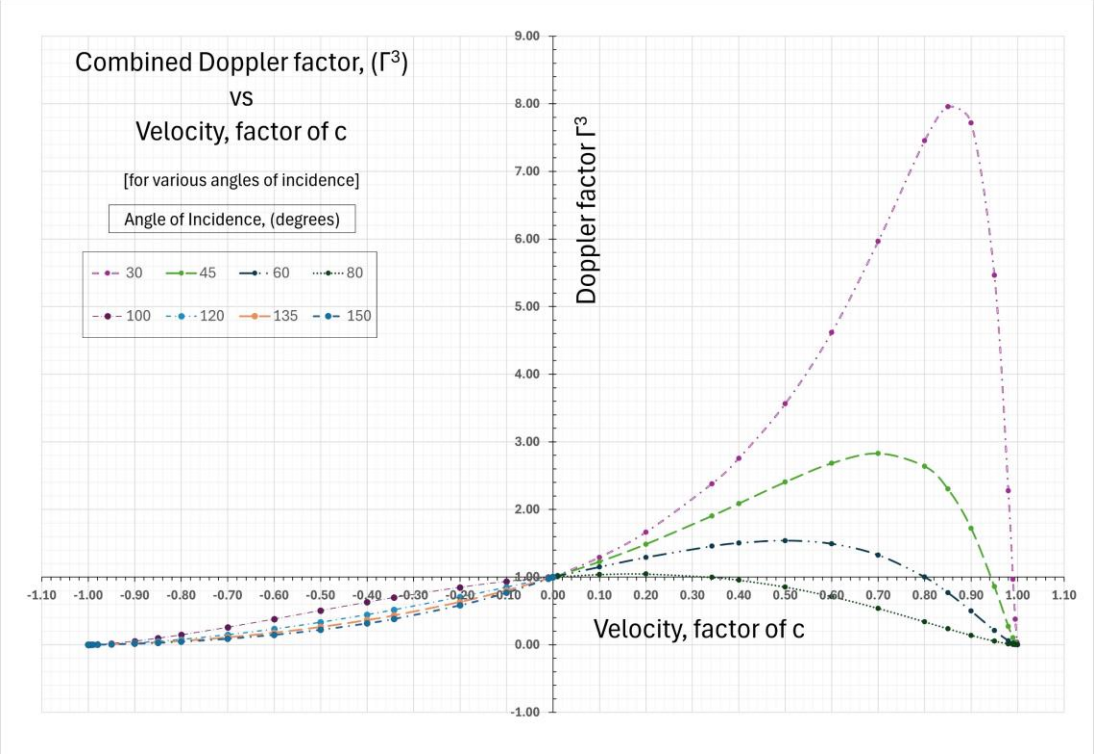

***Graph 1**: The combined Γ^3 Doppler factor, $\gamma^{-3}\left(1-\cos\theta\frac{v}{c}\right)^{-3}$, versus the velocity factor of c for select degrees of angle of incidence. The factors reach a maximum value of $1/(1-\cos^2\theta)^{\frac{3}{2}}$ at $c.\cos\theta$, then decay towards zero.*

8. Relativistic Doppler rotation

The relativistic beaming and aberration effect alters the location of the Center of Gravitation, COG, of a moving or rotating frame, as shown in Fig. 1 & 3. In Fig. 1, the moving rod mass elements approaching the gravitating mass experience an increased gravitational impulse rate and amplitude and the moving rod mass elements which are already receding from the gravitating mass experience a reduced gravitational impulse rate and amplitude. Although it is predicted with Newtonian gravity that the lengthy rod of Fig. 1 would experience a CW rotation before reaching the perpendicular centerline and a CCW rotation after completely passing the centerline, there should be no rotation or movement of the COG from the rod's spatial COG when centered; *owed to symmetry*. However, with Doppler effects applied, directional force symmetry is broken and there is movement of the COG even at the midpoint of passage.

As consequence of the unequal force on either side of the spatial centerline of the relativistic rod, the test mass will be attracted towards to the *COG - moving frame*, in the -X direction as indicated. The relativistic rod will experience torque and rotation due to its displaced COG even at the midpoint of passage; which is not the case for static gravity.

8.1 Example 1

Consider *the mass elements of the thin relativistic rod spanning 2,000 m as depicted in Fig. 2, moving at 0.50 c in the +X direction forming an angle of 45 degrees either side of the gravitating mass located on the centerline as established prior; 10,000 kg and offset 1000 m perpendicular to the rod's motion.*

Eq. 14 is used to establish the COG of gravitational intensity in the ¯Y direction of the rod. Aberration is considered in the $\vec{I}_{gd(y)}$ vector as the direction of the impulses received by the moving rod mass elements do not align with the emission angles of the gravitating mass frame; the direction of the gravitating action is rotated forward, changing slightly the COG calculation.

For COG determination; $$\bar{x}_{cm} = \frac{\sum_i^n \Gamma_i^3 \, x_i \, m_i}{\sum_i^n \Gamma_i^3 m_i} \qquad (16)$$

The result from a multi-point Riemann summation is that the centered rod will experience a COG displacement resulting in a CCW torque and rotation about the displaced COG, approximately 217 m from the rod center as indicated.

9. Rotational gravitational anisotropy

Of particular interest is the gravitomagnetic-like effects of a rotating spherical mass due to relativistic Doppler and Doppler beaming effects.

In non-rotating symmetric spherical masses, the center of gravitation is generally taken to be the spatial center of mass. However, the Center of Gravitation, COG, sensed by a test mass at some distance from a relativistic rotating mass is displaced, as the vectored momentum elements are not directionally equivalent, and differ in magnitude and direction between hemispheres. The vectorial momentum component of the infinitesimal mass elements either receding or approaching must be considered in the energy content of their particular hemispheres as indicated in Eq. 2 & 3. It is then expected that if these vectored linear momentum infinitesimals are integrated, there will be both a difference in gravitational flux intensity between the approaching and receding hemispheres and a shift in the COG towards the Y_1 direction as indicated in Fig. 3. A shift in COG of rotating spheres or rings is consequential to precessional behavior, as discussed in Section 12.

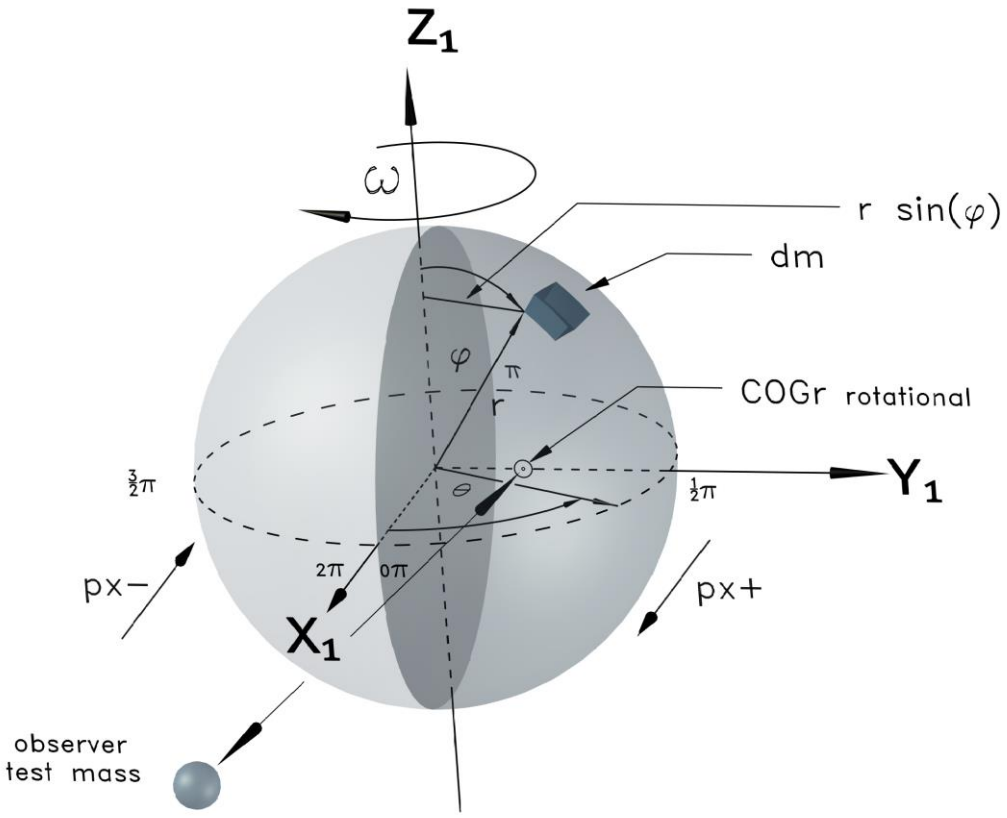

Figure 3: *A spherical mass divided into two hemispheres with a clockwise rotation. The test mass is attracted to the displaced Center of Gravity, [COG$_r$ rotational] on the Y_1^+ axis of the rotating sphere due to the increase in the ρ_{X+} momentum elements in the right hemisphere, and the subtraction of the ρ_{X-} negative momentum elements in the left hemisphere. This effect is exacerbated when Doppler beaming effects are considered.*

9.1 Optical analogy

The frequency shifts for rotating light emitting spheres, in relation to an observer at some distance away on the rotating equatorial plane would see a blue shift in the received light from the hemisphere, whose mass elements have positive momentum vectors towards the observer. The receding hemisphere would have its emitted frequencies red shifted.

As the wave amplitude incremental due to the relativistic beaming effect are not quantified by an interferometer, it is inferred that such an effect, albeit minute, exists and would suggest a brighter equatorial edge on the sun's hemisphere that is rotating towards the observer.

Aligning with the postulate herein, *the Relativistic Anisotropy of Vectored Momentum*, it is expected that the gravitational impulse from the hemisphere mass elements rotating towards an observer are augmented but diminished from the hemisphere mass elements rotating away. There is a Doppler directional gravitational intensification surrounding the equatorial plane and a reduction of intensity on the polar axes.

As a consequence, in relation to the co-located test mass and observer at some distance away on the X_1 axis, the center of gravity of the rotating sphere is no longer sensed to be at the spatial center of the sphere as it would be when not in rotation. Consequently, a test mass falling towards a rotating mass near the equatorial plane would veer towards the displaced location of the COG. This, to an offset observer would appear as if there was a hidden force acting on it at 90 degrees; resembling a Lorentz-like effect. However, it is not; rather a direct inline Newtonian attraction associated with the Amperian motion of mass elements.

10. Center of momentum of the non-rotating hemispheres

Starting with the basic formula to determine the *Center of Mass of the right hemisphere,* COM_{rh}*;*

$$COM_{rh} = \frac{\int \tilde{y}\, dm}{\int\ dm} = \frac{\int \tilde{y}\, \rho\, dv}{\int\ \rho\, dv}$$

$$y = r\ sin\varphi\, sin\theta, \quad dm = \rho\, dv$$

$$dv = r^2\, sin\varphi\, dr\, d\varphi\, d\theta$$

$$COM_{rh} = \frac{\int_0^{\pi}\int_0^{\pi}\int_0^{r} \rho\, r^3\, sin\varphi^2\, sin\theta^1 dr\, d\varphi\, d\theta}{\int_0^{\pi}\int_0^{\pi}\int_0^{r} \rho\, r^2\, sin\varphi\, dr\, d\varphi\, d\theta} = \frac{3r}{8} \qquad (17)$$

10.1 Approximation of the COM^{ρ}, of the non-rotating hemispheres -

Now to approximate by how much the observed center of momentum would be displaced due to vectored momentum elements in a rotating sphere as observed from a distant location on the equatorial plane on the X_1 axis.

The COM^{ρ} for the rotating hemispheres will be approximated by integration using spherical coordinates and tangential momentum infinitesimals rather than angular momentum infinitesimals.

To find the X_1 vector momentum components of the rotating mass elements, the tangential velocity, v, must be factored by $\boldsymbol{sin\,\theta}$ to find v_x. The dm is factored by v_x to obtain dmv_x;

$$v = (\omega\, r\, sin\varphi)$$

$$v_x = (\omega\, r\, sin\varphi\, \boldsymbol{sin\,\theta})$$

$$dmv_x = \rho\, dv\, (\omega\, r\, sin\varphi\, \boldsymbol{sin\,\theta})$$

$$COM^{\rho}{}_{rh} = \frac{\int \tilde{y}\ dmv_x}{\int\ dmv_x} = \frac{\int_0^{\pi}\int_0^{\pi}\int_0^{r} (\, r\sin\varphi\ \sin\theta\,)\,\rho\,(\,r^2\sin\varphi\,)\,(\,\omega\, r\sin\varphi\ \mathbf{sin\,\theta}\,)\,dr\,d\varphi\,d\theta}{\int_0^{\pi}\int_0^{\pi}\int_0^{r}\ \rho\,(\,r^2\sin\varphi\,)\,(\,\omega\, r\sin\varphi\ \mathbf{sin\,\theta}\,)\,dr\,d\varphi\,d\theta} \qquad (18)$$

$$COM^{\rho}{}_{rh} = \frac{\omega\,\rho\int_0^{\pi}\int_0^{\pi}\int_0^{r}\ r^4\,sin^3\varphi\ sin^2\theta\ \ dr\,d\varphi\,d\theta}{\omega\,\rho\int_0^{\pi}\int_0^{\pi}\int_0^{r}\ r^3 sin^2\varphi\ sin^1\theta\ \ dr\,d\varphi\,d\theta} = \frac{8r}{15} \qquad (19)$$

For the *non-rotating left hemisphere*, the $COM^{\rho}{}_{lh}$ would be $-\frac{8r}{15}$ on the Y_1^- axis when integrating from $\pi\ to\ 2\pi$. Thus, as expected, the $COM^{\rho}{}_{sphere}$ of the non-rotating sphere is at its spatial center.

It is calculated that the *Center of Momentum,* $COM^{\rho}{}_{rh}$, of the rotating sphere is not in the same position as when not rotating. The momentum vectors on the hemisphere moving toward the observer add to its relative energy as per Eq. 2, while the hemisphere moving away from the observer loses relative energy as per Eq. 3. Gravitational flux is a factor of this energy and is to be similarly accounted for.

11. Center of momentum of the rotating hemispheres with Γ^3 Doppler factor

Now to integrate the relativistic Doppler factor, Γ^3, with the infinitesimal momentum elements vectored towards the X_1 direction.

Relativistic Doppler vectored momentum, ρ_d, of the hemisphere; without aberration;

$$COM^{\rho d}{}_{rh} = \frac{\omega\,\rho\int_0^{\pi}\int_0^{\pi}\int_0^{r}\ \Gamma^3\ r^4\,sin^3\varphi\ sin^2\theta\ \ dr\,d\varphi\,d\theta}{\omega\,\rho\int_0^{\pi}\int_0^{\pi}\int_0^{r}\ \Gamma^3\ \ r^3\,sin^2\varphi\ \ sin^1\theta\ \ dr\,d\varphi\,d\theta} \qquad (20)$$

Note: *For straight line encounters as per Fig. 1, the Doppler Γ^3 factor uses the cosine of the angle between the source and the observer, however, for compatibility with the spherical coordinate convention as presented in Fig. 3. The cosine must be changed to a sine function in the Γ^3 factor for the rotational scenario pictured; as this function must register "one" when the mass infinitesimal momentum vector is aligned towards the test mass and at its maximum value; which for Fig. 3 is effectively at sin($\pi/2$).*

$$COM^{\rho d}{}_{rh} = \frac{\omega\,\rho\int_0^{\pi}\int_0^{\pi}\int_0^{r}\ \gamma^{-3}\left(1-\mathbf{sin}\,\theta\frac{v}{c}\right)^{-3}\ r^4\,sin^3\varphi\ sin^2\theta\ \ dr\,d\varphi\,d\theta}{\omega\,\rho\int_0^{\pi}\int_0^{\pi}\int_0^{r}\gamma^{-3}\left(1-\mathbf{sin}\,\theta\frac{v}{c}\right)^{-3}\ r^3\,sin^2\varphi\ \ sin^1\theta\ \ dr\,d\varphi\,d\theta} \qquad (21)$$

$$COM^{\rho d}{}_{rh} = \frac{\omega\,\rho\int_0^{\pi}\int_0^{\pi}\int_0^{r}\frac{\left(1-\frac{(\omega\, r\ sin\,\varphi)^2}{c^2}\right)^{\frac{3}{2}}}{\left(1-\mathbf{sin}\,\theta\frac{\omega\, r\ sin\,\varphi}{c}\right)^3}\ r^4\,sin^3\varphi\ sin^2\theta\ \ dr\,d\varphi\,d\theta}{\omega\,\rho\int_0^{\pi}\int_0^{\pi}\int_0^{r}\frac{\left(1-\frac{(\omega\, r\ sin\,\varphi)^2}{c^2}\right)^{\frac{3}{2}}}{\left(1-\mathbf{sin}\,\theta\frac{\omega\, r\ sin\,\varphi}{c}\right)^3}\ r^3\,sin^2\varphi\ \ sin^1\theta\ \ dr\,d\varphi\,d\theta} \qquad (22)$$

Solving using Python numeric processing to find the perceived barycenter of the of $COM^{\rho d}{}_{rh}$ & $COM^{\rho d}{}_{lh}$ using earth mass and radius, but with an improbable angular velocity of $\omega = 24.0\ rads/sec$, (v=0.51c at the equator), the perceived equatorial Center of Momentum, $COM^{\rho d}{}_{earth}$ has moved approximately 2,889,293 m away from the spatial center; 0.45350647 the radius of the earth.

Solving for the earths sidereal rotational angular velocity, $\omega = 7.29212e^{-5}\ rads/sec$, ($v_t$ = approx. 465.1 m/s at the equator) the Center of Momentum, $COM^{\rho d}{}_{earth}$ has moved 9.87 m away from the spatial center; essentially imperceptible.

As the Doppler factors concentrate the mass element's gravitational flux tangentially in the direction of rotation, the gravitational intensification is seen to be most pronounced surrounding the equatorial plane and most diminished on the polar axis.

The Z axis attenuation is attributed to the constraint that all infinitesimal tangential momentum vectors of the rotating sphere become 90 degrees to the Z axis when the rotating mass elements approach **c**.

12. Relativistic precession of rotating objects

In the diagram below, the anisotropic Doppler gravitational effects on the precession of the relativistic rotating rings in close proximity is observed by the development of precession on each rotating ring.

The consequence of the relativistic Doppler displacement of the COGs of the rotating rings as indicated in Fig. 4, allows for torque to appear on all three axes; which is not present for non-rotating rings.

The magnitude of procession and acceleration is linked to the displacement of the COGs, which in turn is linked to the ring angular velocity, ring mass and geometry.

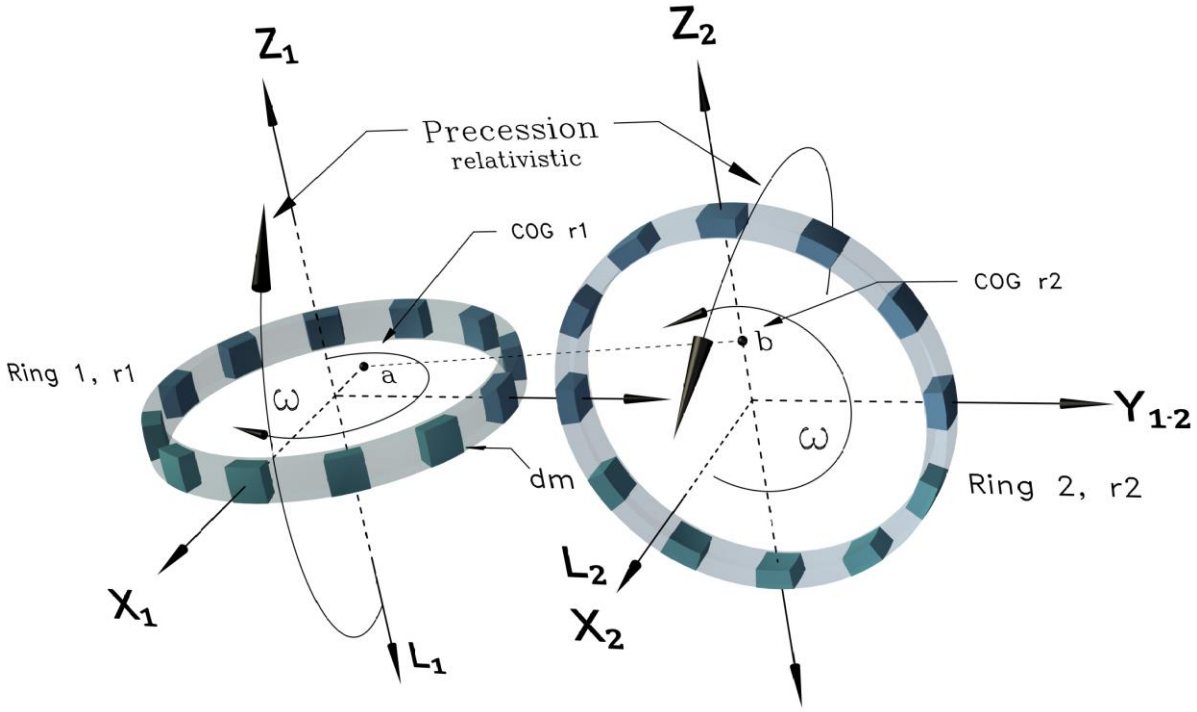

***Figure 4**: A depiction of rotating rings in close proximity showing the relativistically Doppler displaced COG, points a and b; (exaggerated). As the displaced COGs are not centered on the spatial centers, there is an intensification of the gravitational force displaced from the spatial centers, resulting in torque and complex precession on all three axes.*

At the instant pictured in the mockup, there is precession on the X_1, Y_1, Y_2, Z_2 axes with angular acceleration for L_1 and L_2 for Rings 1 and 2 respectively. Intuitively, it is expected that these rings will, at some point reach stability with angular momentum vectors L_1 and L_2 co-aligning in one direction.

There still remains the circumstance of the continued torque and angular acceleration about the aligned principal axes, L_1 and L_2. Considering the rotational form of Newtons 3rd law, the continued torque on the displaced $COM^{\rho d}{}_{r1\&r2}$ will impose an angular impulse equivalently on each ring resulting in continued acceleration of the rings;

$$J_{r_{1a}-r_{2b}} = J_{r_{2b}-r_{1a}} \tag{23}$$

If the energy for rotational acceleration is extracted from a re-alignment of gravitational forces on the rings, do the rings slow their fall towards each other when the COG displacements from the spatial center approach their radii? The behavior of a yo-yo comes to mind; gravitational energy is converted into angular velocity as the yo-yo falls at a reduced velocity as torque is applied via a displaced moment arm.

Where τ_{r_1} is the torque applied to Ring 1.

$$\tau_{r_1} \cong I_{gd_{r2}}.m_{r1}.COG_{dr1} \quad \left[\frac{Kg\ m^2}{s^2}\right] \qquad (24)$$

These Doppler gyroscopic processional interactions require additional investigation.

13. Discussion and summary

Using Gauss's flux theorem in conjunction with relativistic Doppler theorem allows for the re-distribution and intensification of vectored gravitational flux from a Gaussian surface. This allows for a better estimation of the gravitational intensity present in a region of space being influenced by moving masses.

The asymmetric outward projection and focusing of gravitational flux and intensity surrounding relativistic rotating masses increases the gravitational response around the equatorial planes and diminishes it at the poles.

The Doppler $COM^{\rho}{}_{sphere}$ of the rotating sphere, Fig. 3 is linked to angular velocity and causes a laterally outward displacement on the hemisphere rotating towards the test mass. This causes a veering from the expected trajectory of the infalling test mass away from the spatial center of the sphere. This effect, feigning as a Lorentz-like force, can alternatively be explained by applying the Doppler-Gaussian flux theorem to Amperian motion. Although it is found to be quite insignificant for earth's rotation velocity, it may be relevant elsewhere.

The displaced center of gravity of relativistic rotating rings in Fig. 4 causes precession on all three axes; an effect that is not present when applying static gravity models. For the case shown, it is expected that at some point, the rings would achieve stability when the principal axes co-align, a tendency observed in planetary systems.

The application of the Doppler Gravitational effect to galactic rotation, as developed in Section 6, which increased gravitational intensity outside and forward of a large collection of rotating objects, increases the gravitational gradient incrementally as the distance from the galactic center increases, and would result in anomalous orbital behavior.

For relativistic blazars, the intensification of the gravitational effect within its Doppler focused cone due to the high jet velocity of cumulative ejected mass would cause anomalous jet deceleration and collimation of previously expelled mass elements in line with the jet; while similarly being attracted towards the already expelled mass; reversing the tendency beyond the center of mass of the jet.

It is noted that in the case of an emitting source in circular orbit around a stationary receiver; the central observer will see the energy "red-shifted"; *giving the impression that the source was travelling away from the receiver*.

A case of a rod passing a gravitating mass was presented at its midpoint during its passage, Example 1. Although not fully evaluated over the entire trajectory, it was simply to highlight the existence of a significant Doppler rotational effect where spatial symmetry and static gravitation would suggest none.

14. References

[1] Heaviside, O. (1893). *Electromagnetic Theory, a Gravitational and Electromagnetic Analogy.* London: The Electrician Printing and Publishing Co. Vol. 1, Appendix B, Part II, 463–466.

[2] de Broglie, L. V. (1925). *On the Theory of Quanta*. A translation of: Recherches Sur La Théorie Des Quanta. Annales de Physique, 10^{e} Serie, Tome III, by A. F. Kracklauer.

[3] Einstein, A. (1905). *Zur Elektrodynamik bewegter Körper*. Annalen der Physik, 322, 891-921. https://doi.org/10.1002/andp.19053221004

[4] Doppler, C. (1847). *Über den Einfluss der Bewegung des Fortpflanzungsmittels auf die Erscheinungen der Äther, Luft und Wasserwellen, Ein weiterer Beitrag zur allgemeinen Wellenlehre*. Prag: Bernard Bolzano & In Commission bei Borrosch & André.

[5] Planck, M. (1906). *The Principle of Relativity and the Fundamental Equations of Mechanics*. A translation of: *Das Prinzip der Relativität und die Grundgleichungen der Mechanik*. Verhandlungen Deutsche Physikalische Gesellschaft, 8, 136–141. by Wikisource. https://en.wikisource.org/wiki/Translation:The_Principle_of_Relativity_and_the_Fundamental_Equations_of_Mechanics

[6] Johnson, M. H. & Teller, E. (1982). *Intensity changes in the Doppler effect.* Proceedings of the National Academy of Sciences (PNAS), Vol. 79, Issue 4, 1340.

[7] *Gauss's law for gravity*. (2025, September 8). In *Wikipedia*. https://en.wikipedia.org/wiki/Gauss's_law_for_gravity

[8] Vestergaard Schmidt, M. (2023*). On the connection between the magnetic part of electromagnetic radiation and the Doppler amplitude shift*. OSF preprints. https://doi.org/10.31219/osf.io/wn3br

[9] Doppler, C. (1842). *Über das farbige Licht der Doppelsterne und einiger anderer Gestirne des* Himmels. Prag: In Commission bei Borrosch & André.

[10] Kellermann, K. I., & Verschuur, G. L. (1988). *Radio Galaxies and Quasars*. Galactic and Extragalactic Radio Astronomy (2nd ed). Springer-Verlag, New York, 563. https://link.springer.com/book/10.1007/978-1-4612-3936-9

[11] López Arias, V. E. (2019). *Doppler boosting effects on relativistic jets*. Facultat de Física, Universitat de Barcelona, Spain. https://hdl.handle.net/2445/141526

[12] Homan, D. C., Lister, M. L., Kovalev, Y. Y., Pushkarev, A. B., Savolainen, T., Kellermann, K. I., Richards, J. L., Ros, E. (2015, January 10). *MOJAVE. XII. Acceleration and Collimation of Blazar Jets on Parsec Scales*. The Astrophysical Journal, Vol. 798, Number 2, Article 134. https://iopscience.iop.org/article/10.1088/0004-637X/798/2/134

[13] Jet Propulsion Laboratory, Nasa. *Planetary Physical Parameters*. *2008. viewed January 11, 2026.* https://ssd.jpl.nasa.gov/planets/phys_par.html

Appendix 1

As validation for evaluating with spherical coordinates, estimates were made against known physical and rotational data of the earth [13]; angular kinetic energy and angular momentum.

Input values – earth: $\mathrm{R}_e = 6{,}371{,}008\ \mathrm{m},\ \omega = 7.29212e^{-5}\frac{rads}{s}$

Density factors ρ, kg/m³ : $\rho_{average} = 5{,}513.4$ or $\rho_{variable} = \left(14{,}194.65 - 11{,}575\ \left(\frac{r}{R_e}\right)\right)$

Rotational Kinetic Energy

$$Ke_{rot} = \omega^2\ \rho \int_0^{2\pi}\int_0^{\pi}\int_0^{r}\ r^4\ sin^3\varphi\ \ sin^2\theta\ \ dr\ d\varphi\ d\theta$$

$$Ke_{rot} = (7.29212e^{-5})^2\ \rho \int_0^{2\pi}\int_0^{\pi}\int_0^{6371008}\ r^4\ sin^3\varphi\ \ sin^2\theta\ \ dr\ d\varphi\ d\theta \qquad (25)$$

$$Ke_{rot-\rho\ average} = \mathbf{2.5780e^{29}} \qquad Ke_{rot-\rho\ variable} = \mathbf{2.1269e^{29}}$$

Rotational momentum

$$P_{rot} = \omega\ \rho\ \int_0^{2\pi}\int_0^{\pi}\int_0^{r}\ \ r^4\ sin^3\varphi\ \ dr\ d\varphi\ d\theta$$

$$P_{rot} = (7.29212e^{-5})\ \rho \int_0^{2\pi}\int_0^{\pi}\int_0^{6371008} r^4\ sin^3\varphi\ \ dr\ d\varphi\ d\theta \qquad (26)$$

$$P_{rot-\rho\ average} = \mathbf{7.0707e^{33}} \qquad P_{rot-\rho\ variable} = \mathbf{5.8336e^{33}}$$

Doppler's original diagrams

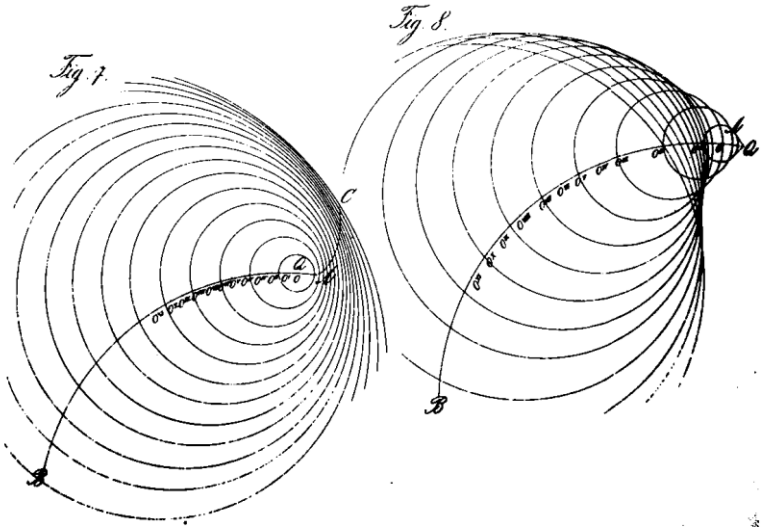

Figure 5*: Doppler's 1847 original diagram illustrating radiating bodies on curved trajectories [4], Fig. 7; below the velocity limit of the medium, Fig. 8; above the velocity limit of the medium. Note the asymmetric accumulation of flux indicated by the directionally compressed wave crests.*